APPROVED FOR PUBLIC RELEASE

[redacted]

UNCLASSIFIED

CIC-14 REPORT COLLECTION
REPRODUCTION
COPY

Classification changed to UNCLASSIFIED
by authority of the U. S. Atomic Energy Commission,
Per Jack H. Kahn List #10 5-10-57
By REPORT LIBRARY M. Chelius
6-21-57

PUBLICLY RELEASABLE
LANL Classification Group
M. Fountain 2/26/96

LA - 555

[redacted]

C.3

May 1, 1946

This document contains 21 pages

NEUTRON EXPERIMENTS WITH BERYLLIUM SPHERES

WORK DONE BY:

M. Camac
E. Creutz
L. Larson
D. Martin
L. Slotin
W. VanBeneden

REPORT WRITTEN BY:

E. Creutz

UNCLASSIFIED

[redacted]

APPROVED FOR PUBLIC RELEASE

APPROVED FOR PUBLIC RELEASE

[redacted] STED

UNCLASSIFIED

ABSTRACT

Neutron distributions were measured in different sizes of Beryllium spheres, using a Polonium-Beryllium source. Various types of foils were employed in an attempt to approximate the spectral distribution.

LOS ALAMOS NATL. LAB. LIBS
3 9338 00330 2014

[redacted]

UNCLASSIFIED

APPROVED FOR PUBLIC RELEASE

APPROVED FOR PUBLIC RELEASE

[redacted] UNCLASSIFIED

NEUTRON EXPERIMENTS WITH BERYLLIUM SPHERES

E. Creutz and L. Creutz

INTRODUCTION.

Because of the interest in beryllium metal for chain-reacting devices, and also because of the availability of a series of beryllium spheres of various sizes, it was considered worthwhile to measure the distribution of neutrons in them when various sources were placed in the centers. Unfortunately, the spectrum of the suitably strong sources available (polonium-alpha-beryllium) is not very well known and is far from homogeneous. However, by using spheres of different sizes and detectors with various thresholds, it was believed some useful information could be obtained.

SECTION I. METHOD

The neutron sources themselves consisted of thin-walled beryllium spheres about .830" O.D. filled with a mixture of Be powder and polonium. The large Be spheres in which the neutron distributions were to be measured, were prepared by drilling a 1" hole to the center. This hole terminated in a spherical cavity to hold the source at the center. A Be tube was filled with Be discs of 1/8" and 1/4" thickness, and foils of various materials useful for neutron detection were sandwiched in between the discs. The source was then dropped in the sphere, and the tube containing the discs and foils were put in place. After a suitable bombardment time, the foils were removed, the induced radioactivity measured in a standard geometry with a Geiger-Mueller counter, and suitable corrections applied for the weights of the foils to give the distribution of the particular neutrons

[redacted] UNCLASSIFIED

APPROVED FOR PUBLIC RELEASE

APPROVED FOR PUBLIC RELEASE

UNCLASSIFIED

absorbed by the foils along the radius of the sphere.

SECTION II. CALIBRATION OF FOILS

In order to measure the counting efficiency of our geometry, the foils were then placed in the large graphite pile in G Building, where the thermal flux has been calculated by R. Walker.

Cadmium differences were taken with the foils in question so that the activation due to the thermal-neutrons was measured. Since the ratio of the activation of the foils out of cadmium to that in cadmium was not very large (about 10) at the position in the pile which was used, the neutrons measured by the cadmium difference method were not very good thermal neutrons. The reason for this is that the cadmium cut-off is somewhat too high. V. Weiskopf suggested comparing the cadmium difference measurement with a gadolinium difference. This was done, shielding the detectors with layers of Gd_2O_3 containing about 8 milligrams per cm^2 of Gd_2O_3. This gave a thermal activity induced in the foils (by difference) about 3½% less than did the cadmium difference. Since it was felt that this value might be on the low side, an average value was taken for the true thermal effect. That is, the thermal effect given by the cadmium difference was reduced by 1.75% before calculating the counting efficiency of our geometry.

SECTION III. CORRECTION FOR ABSORPTION OF BETA RAYS IN FOILS

In order to have the foils fairly easy to handle, they must be several mils thick. In this case there is appreciable absorption of the Beta rays in the foil itself. This effect was studied by measuring the activity of a standard foil in the standard counting geometry and then covering it with successive, thin, non-irradiated foils of the same material to determine the

UNCLASSIFIED

APPROVED FOR PUBLIC RELEASE

APPROVED FOR PUBLIC RELEASE

[redacted] UNCLASSIFIED

absorption coefficient (see Figures 1 and 2). A correction was then made to obtain the actual, specific activity of the foil as follows:

$A_{(x)}$ = Actual activity of foil per unit thickness at depth x in foil.

ε = Observed counting rate from thick foil.

μ = Linear absorption coefficient of foil material for its own Beta rays.

$a = \int_0 A(x)e^{-\mu x}\,dx$, where x is the thickness of the foil.

In a thermal flux, A(x) was found to be nearly independent of the depth in the foil for 5 mil foils. Therefore, $A(x) = \dfrac{a\mu}{1 - e^{-\mu x}}$.

Data for a series of indium foils of various thicknesses are given in Table I. The essential constancy of A(x) computed in this way for foils varying in thickness from 2.3 to 15 mils is additional proof that A(x) is constant throughout the thickness of any one of these foils. This table also shows the fallacy of attaching significance to activity per milligram for foils of varying weights.

SECTION IV. CORRECTION FOR DEPLETION OF NEUTRON DENSITY IN FOIL

It is not satisfactory to assume the efficiency of a foil for detecting neutrons is independent of the spectrum, depending only on some average cross-section. The reason is that those neutrons whose energy is such that they are very readily absorbed by the foil atoms will almost completely disappear in the surface layers of the foil, and the atoms inside the foil might as well not be there. The effective weight of the foil is thus less than its own true weight.

The magnitude of this effect will depend on the actual spectrum, but for this experiment only two kinds of spectra were considered. Namely, the

[redacted] UNCLASSIFIED

APPROVED FOR PUBLIC RELEASE

APPROVED FOR PUBLIC RELEASE

[redacted] UNCLASSIFIED

thermal neutrons in the graphite pile, and the total neutrons in a beryllium sphere. Actually, the spectrum in a beryllium sphere depends (as well as on the source, which in these experiments was standard) on the size of the sphere and the position in it. For making this correction, a standard neutron spectrum was chosen as the "spectrum in beryllium"; i.e., that which existed at $2\frac{1}{4}$" from the center of the 13-11/16" sphere. The distribution of neutrons within a foil embedded in this spectrum was obtained by piling up several very thin foils to obtain a total thickness equal to one of the regular 5 mil foils. After bombardment, this sandwich of foils was taken apart, and each one of the thin parts counted for induced activity. This activity was then compared with that in a very thin foil placed in the same spectrum. This foil was so thin (.0005"-.001") that the correction for depletion of the beam in it was assumed negligible. (An estimate shows this correction to be less than 5%, and it is only a correction to another correction.)

It was found that this depletion correction was unimportant (less than 5%) with 5-mil indium and gold foils in the thermal flux (see also Section III). However, in the beryllium sphere flux, it was large--of the order of 40%.

Figures 3 and 4 show the distribution of activity in gold and indium 5-mil foils compared to the activity of a thin foil.

It was found that the activity distribution curve in the foil could be fitted well within the experimental limitation by a single hyperbolic cosine. The relative counting efficiencies in thermal flux and beryllium sphere flux were thus calculated.

$$\frac{E_{th}}{E_{Be}} = \frac{\int_0^{\quad} \quad dx}{\int_0^{\quad} \quad dx} = \frac{\quad}{\quad}$$

[redacted] UNCLASSIFIED

APPROVED FOR PUBLIC RELEASE

APPROVED FOR PUBLIC RELEASE

UNCLASSIFIED

Using the values of α, β and γ, found experimentally and listed below,

	α	β	γ
Indium	.535	.305 mil^{-1}	.542 mil^{-1}
Gold	.570	.326	1.13

the ratio of efficiency was found to be 1.14, both for indium and for gold. For lack of better information, it was then assumed to be the same for 25 and manganese. This is probably too high for manganese, since γ should be smaller; but since α and β were not determined, nothing can be done about it until more experiments are carried out.

SECTION V. EXPERIMENTAL DATA

The data on resonance detectors are given in Table II and in Figures 5, 6, and 7. The columns in Table II are explained as follows.

(1) Location of detector. For calibration, the detector was in a graphite pile; and in this case the cadmium difference was reduced by 1.75%, to correct for the rather high cadmium cut-off, and used to obtain Column 3. When the detector was in a beryllium sphere, it was placed .480" from the center. The diameter of the source sphere was .830".

(2) The element used as detector.

(3) In thermal flux, this is the number of clicks of the mechanical counter per minute per milligram of material corrected to saturated activity. (In the case of 25, the activity was read at a standard time after the end of a standard bombardment. That is, 114 minutes after a bombardment of 21 hours, three minutes.) Since the same units are used in computing the activity in the beryllium sphere flux, they cancel out and are not important. The weight correction is small, since all foils of a given material were the same within a few percent. The self-absorption of the foils (necessary since the neutron distribution in them is different in the thermal and the beryllium sphere flux) is taken

UNCLASSIFIED

APPROVED FOR PUBLIC RELEASE

APPROVED FOR PUBLIC RELEASE

[redacted] UNCLASSIFIED

care of by the method described in Section III.

(4) The thermal cross-section, as found in Los Alamos Handbook.

(5) The thermal flux in the graphite pile calculated by R. Walker at the point used for calibration.

(6) Relative foil efficiency for thermal and beryllium sphere fluxes discussed in Section IV.

(7) Product of Columns 4 and 5.

(8) Observed counting rate of foil placed .480" from center of sphere in question. Corrected to saturated activity and calculated for a total source strength at the center of 10^7 neutrons per second. Correction was made for the decay of the source. Two sources were used; the weaker (5.20) was measured by Slotin. The stronger was compared to this by counting indium induced activity when first one source and then the other was placed in the 6" beryllium sphere. Figure 9 shows the strength of each source calculated as function of the time.

(9) This is an average product of the flux and the cross-section for all neutrons absorbed by the foil in question. It is given per unit source strength. The units of this quantity are (flux barns) per (neutron per second). These are calculated as follows:

$$\left(\frac{\text{clicks}}{\text{min. mg}}\right)_{th} = (n v \sigma)_{th}\ \text{Eff}_{th}$$

$$\frac{1}{\text{Source strength}}\left(\frac{\text{clicks}}{\text{min mg}}\right)_{Be} = \frac{1}{(n v \sigma)_{Be}} \cdot \text{Eff}_{Be} \cdot \left(\frac{1}{\text{Source strength}}\right)$$

$$\frac{\frac{1}{(n v \sigma)_{Be}}}{\text{Source strength}} = \frac{\left(\frac{\text{Clicks}}{\text{Min/Mg}}\right)_{Be}}{\left(\frac{\text{Clicks}}{\text{Min/Mg}}\right)_{Th}} \cdot \frac{\text{Eff}_{Th}}{\text{Eff}_{Be}} \cdot (n v \sigma)_{Th}$$

[redacted] UNCLASSIFIED

APPROVED FOR PUBLIC RELEASE

APPROVED FOR PUBLIC RELEASE

[redacted]

UNCLASSIFIED

Figures 5, 6, and 7 show the distribution of all neutrons absorbed by the foils. The circles represent the measurements with gold, indium, and manganese foils all normalized to unity at the point .480" from the center. There were no significant differences found in the distribution curves given by these three detectors. The triangles show this distribution as measured with 25 foils, normalized to unity at the first point. In all cases this distribution falls off more steeply at the center than does the other.

The squares are the hypo-cadmium neutrons. This data was obtained by subtracting the activity induced in indium foils in cadmium from the total activity. These points are normalized so that the total activity (no cadmium) is unity at .480" from the center. They show, therefore, the ratio of the activity induced in indium by cadmium absorbable neutrons to the total activity induced in indium at that same place. The + 's are the distribution of neutrons producing the (n,p) reaction in phosphorus (threshold ~ 1.5 Mev).

Figure 8 shows the distribution in the 13-11/16" beryllium sphere, of neutrons producing fission in 28, (n,p) in phosphorus and (n,p) in sulphur. Also plotted (x's) is the phosphorus activity times r^2. The positive attenuation shows that the loss of these high energy neutrons by absorption and slowing down is not made up for by (n,2n) in beryllium under these conditions.

Figure 10 shows the value of $\frac{\text{Flux Barns}}{\text{Source}}$ measured .480" from the center of beryllium spheres with various detectors plotted against the sphere diameter.

Figure 11 shows the distribution of neutrons measured with gold detectors in a 3.52" diameter 49 sphere inside a 9" diameter beryllium sphere. A mock-fission source was at the center of the 49 sphere.

[redacted]

UNCLASSIFIED

APPROVED FOR PUBLIC RELEASE

APPROVED FOR PUBLIC RELEASE

UNCLASSIFIED

TABLE II

LOCATION ①	DETECTOR ②	CLICKS MIN - MG ③	$\bar{\sigma}_a$ BARNS ④	ϕ_{th} (n/cm²-sec) ⑤	ϵ_{36} ⑥	ϵ_{Be} ⑦	Σ_{abs} (cm⁻¹)	Watts x 10^7 ⑧	Min. MC Source	Watts/Source ⑨	⑧ X ⑨ X ③ X 10^{-7}
Graphite pile		0932	95.7	13,200	1.44		2.6×10^6				
"	In	6B5	194	13,200	1.44		2.56×10^6				
"	Mn	218	72.8	13,200	(1.44)		$.65 \times 10^6$				
"	25	076	320	13,200	(1.44)		6.85×10^6				
13 Be	Au							.275	.536		
13 Be	IN							.83	0.986		
13 Be	Mn							.442	.482		
13 Be	25							.170	2.21		
9" Be	Au							.123	.241		
9" Be	IN							.642	.345		
9" Be	Mn							.160	.175		
9" Be	25							.055	.713		
6" Be	Au							.0369	.072		
6" Be	IN							.166	.0895		
6" Be	Mn							.0386	.0432		
6" Be	25							.0258	.0334		

UNCLASSIFIED

KEUFFEL & ESSER CO., N. Y. NO. 359-11
MADE IN U.S.A.

APPROVED FOR PUBLIC RELEASE

APPROVED FOR PUBLIC RELEASE

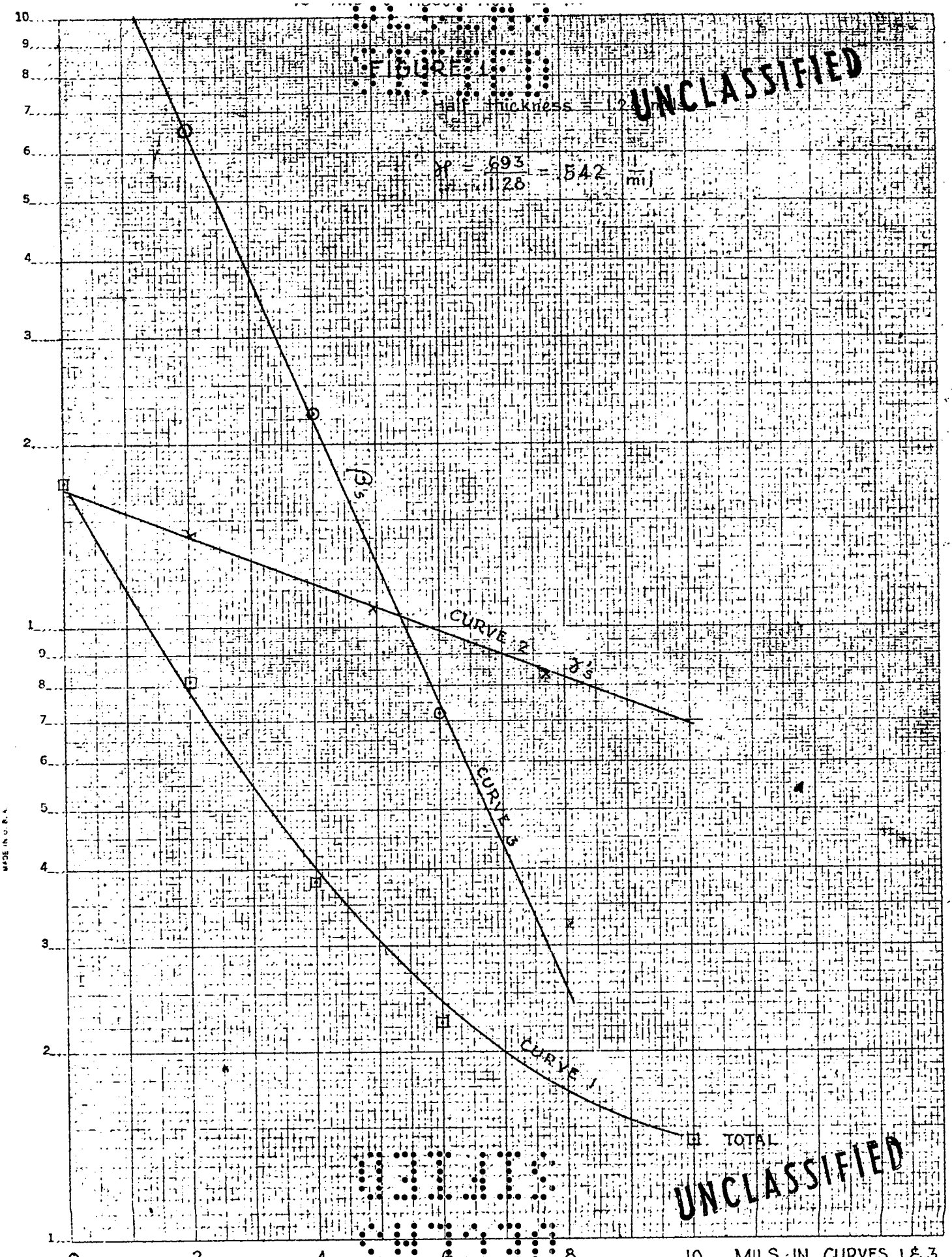

APPROVED FOR PUBLIC RELEASE

APPROVED FOR PUBLIC RELEASE

FIGURE 2

Half thickness = .612 mils

$\mu = \frac{.693}{.612} = 1.13 \frac{1}{mil}$

UNCLASSIFIED

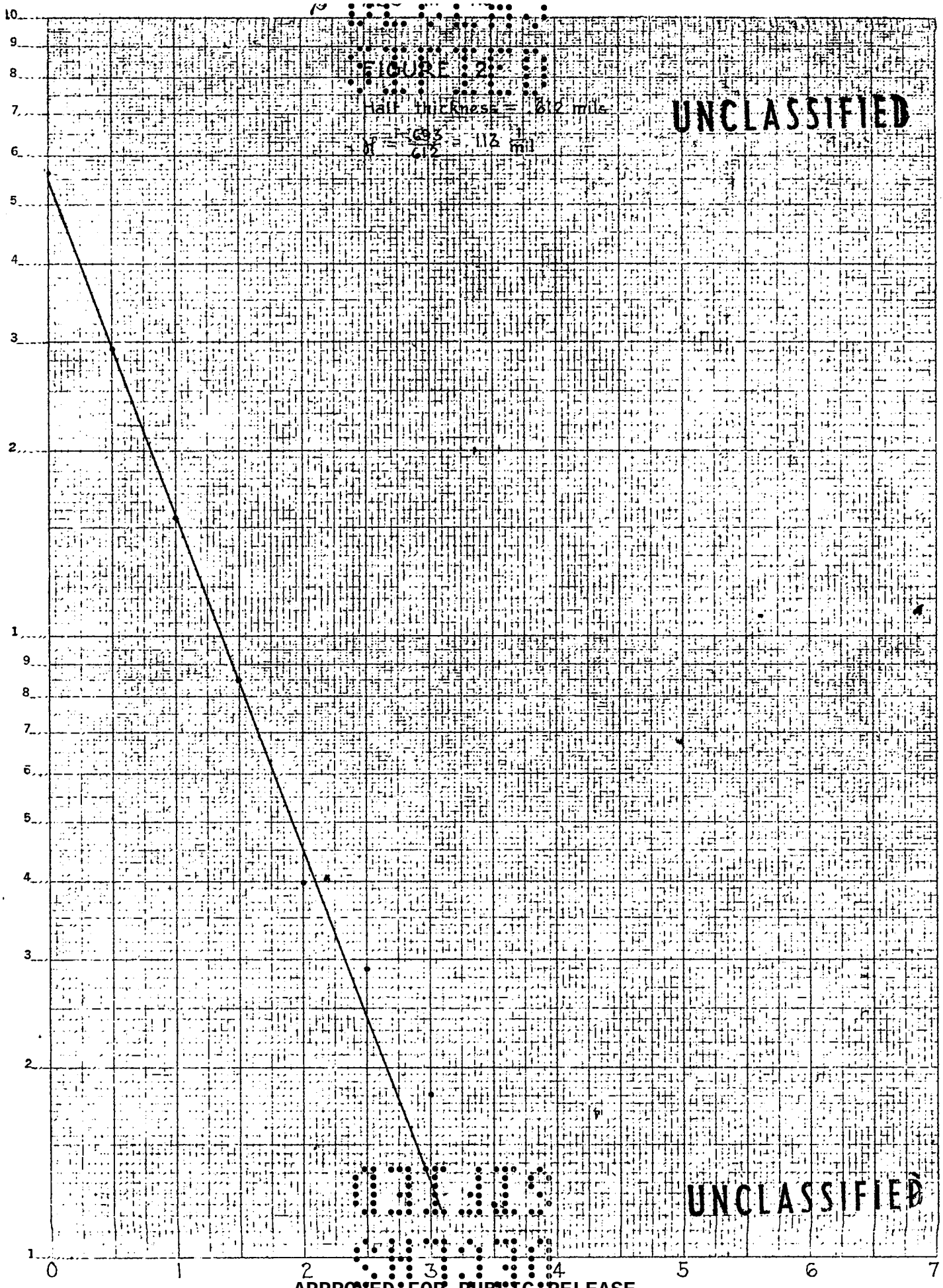

UNCLASSIFIED

APPROVED FOR PUBLIC RELEASE

APPROVED FOR PUBLIC RELEASE

UNCLASSIFIED

FIGURE 3

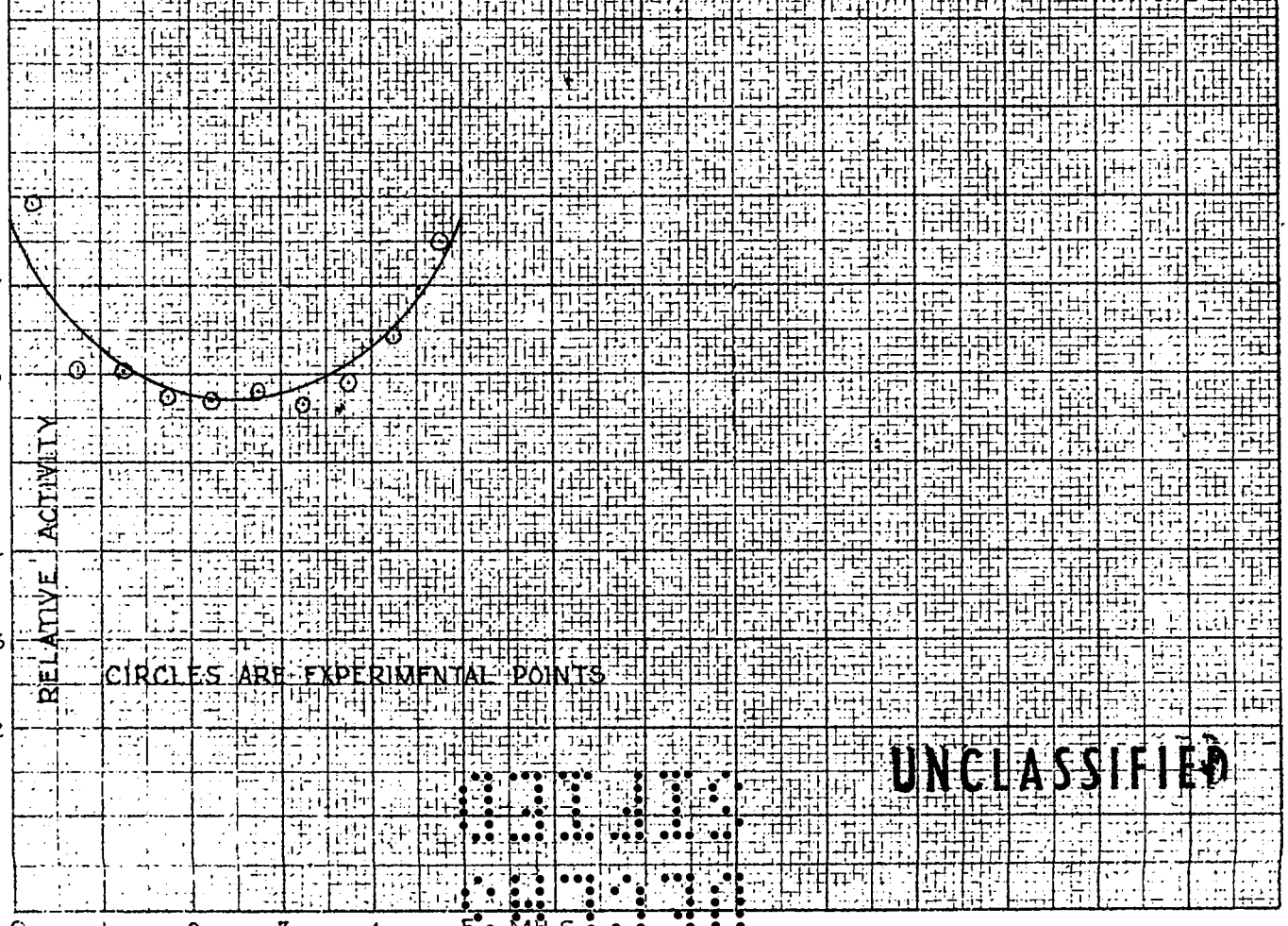

UNCLASSIFIED

APPROVED FOR PUBLIC RELEASE

APPROVED FOR PUBLIC RELEASE

UNCLASSIFIED

FIGURE 4

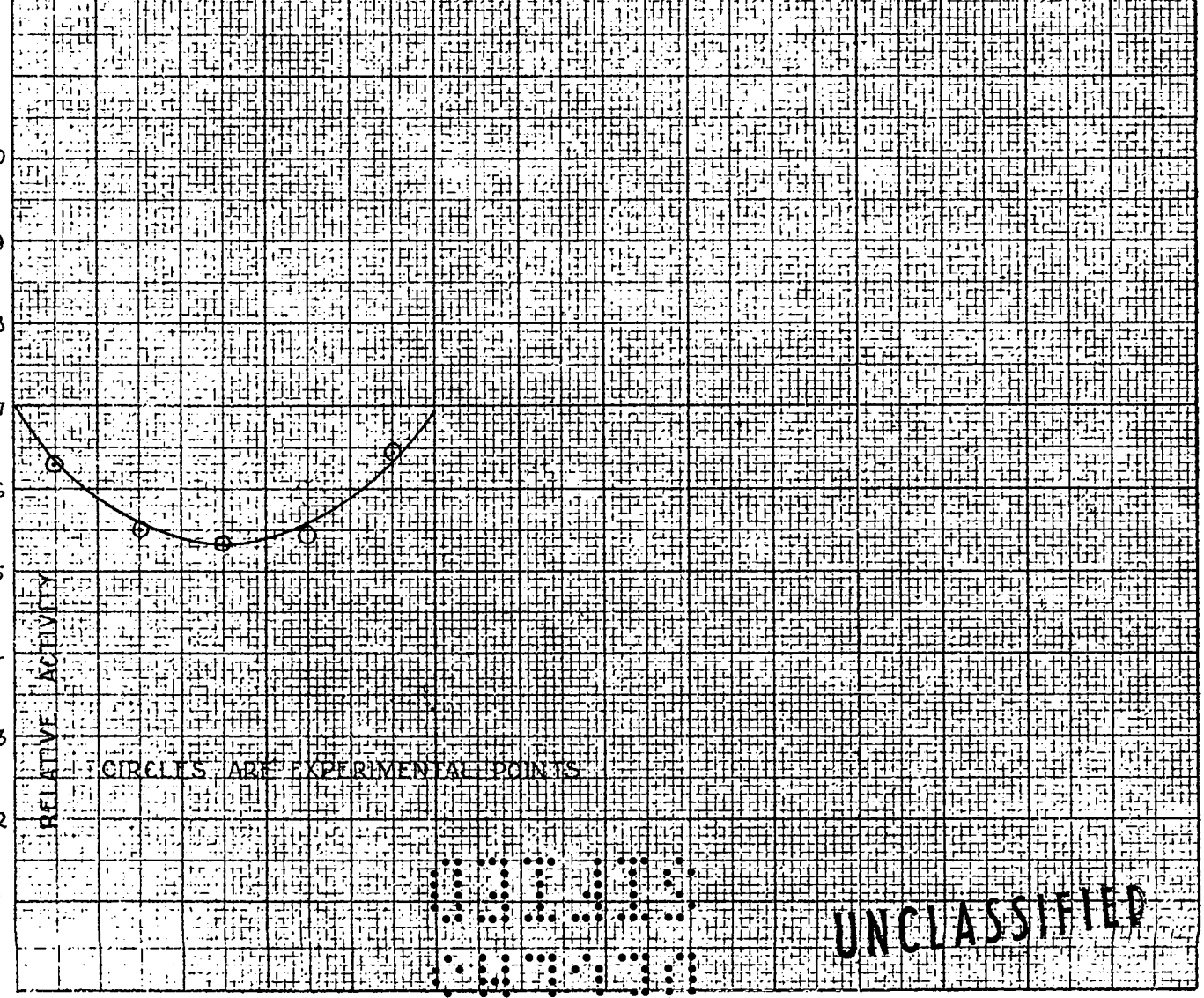

UNCLASSIFIED

APPROVED FOR PUBLIC RELEASE

APPROVED FOR PUBLIC RELEASE

UNCLASSIFIED

FIGURE 5

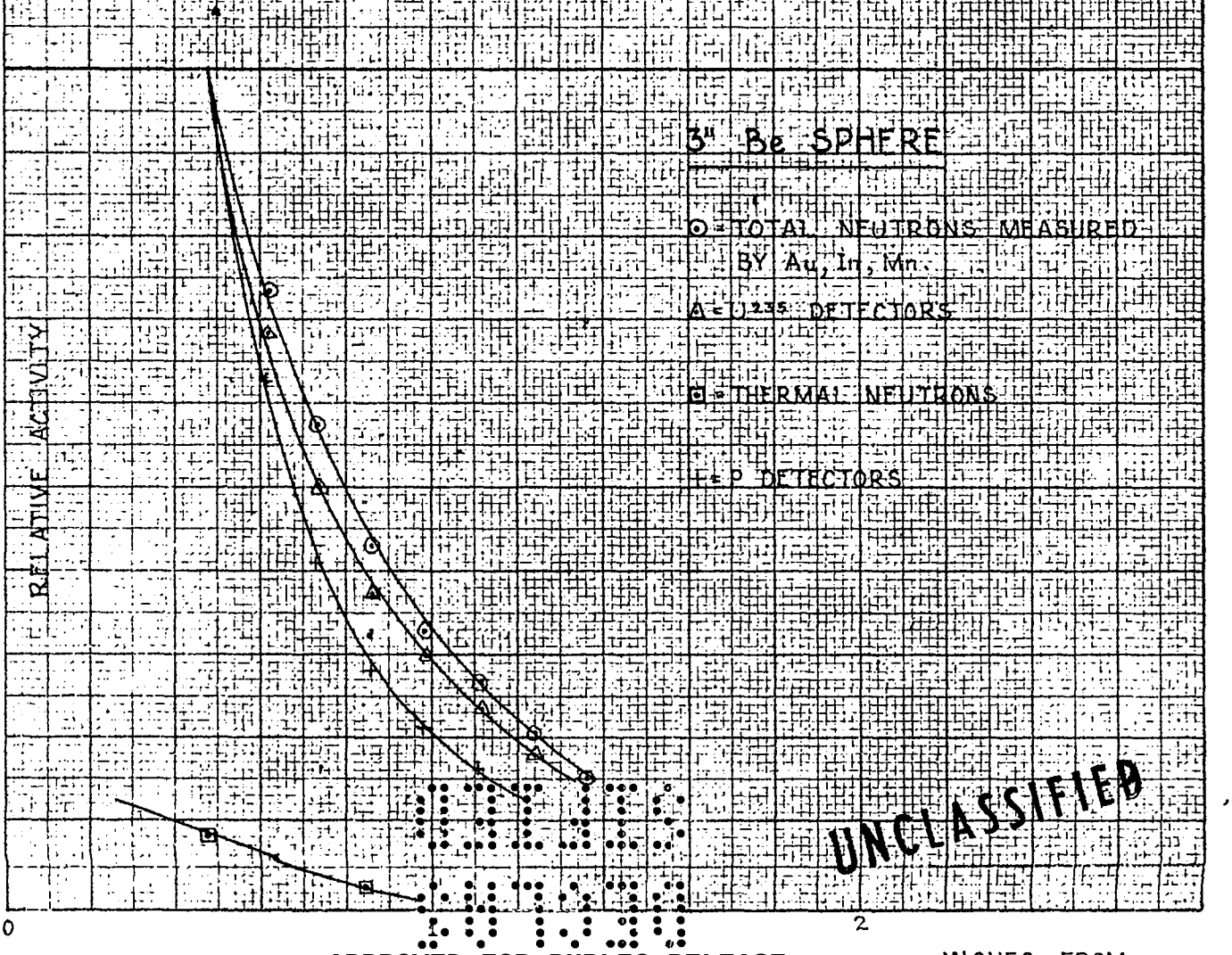

UNCLASSIFIED

APPROVED FOR PUBLIC RELEASE

APPROVED FOR PUBLIC RELEASE

FIGURE 6

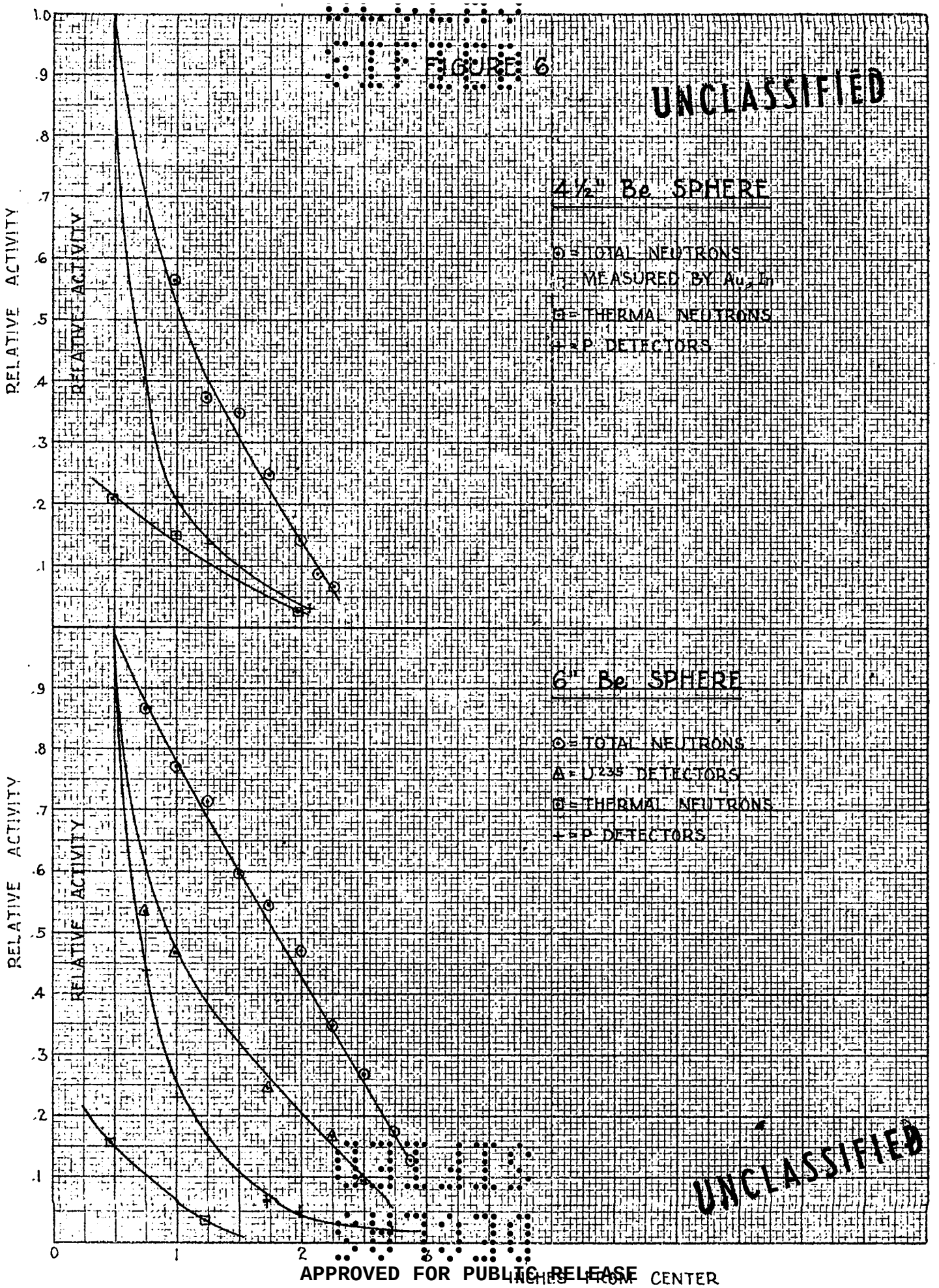

APPROVED FOR PUBLIC RELEASE

APPROVED FOR PUBLIC RELEASE

FIGURE 7

UNCLASSIFIED

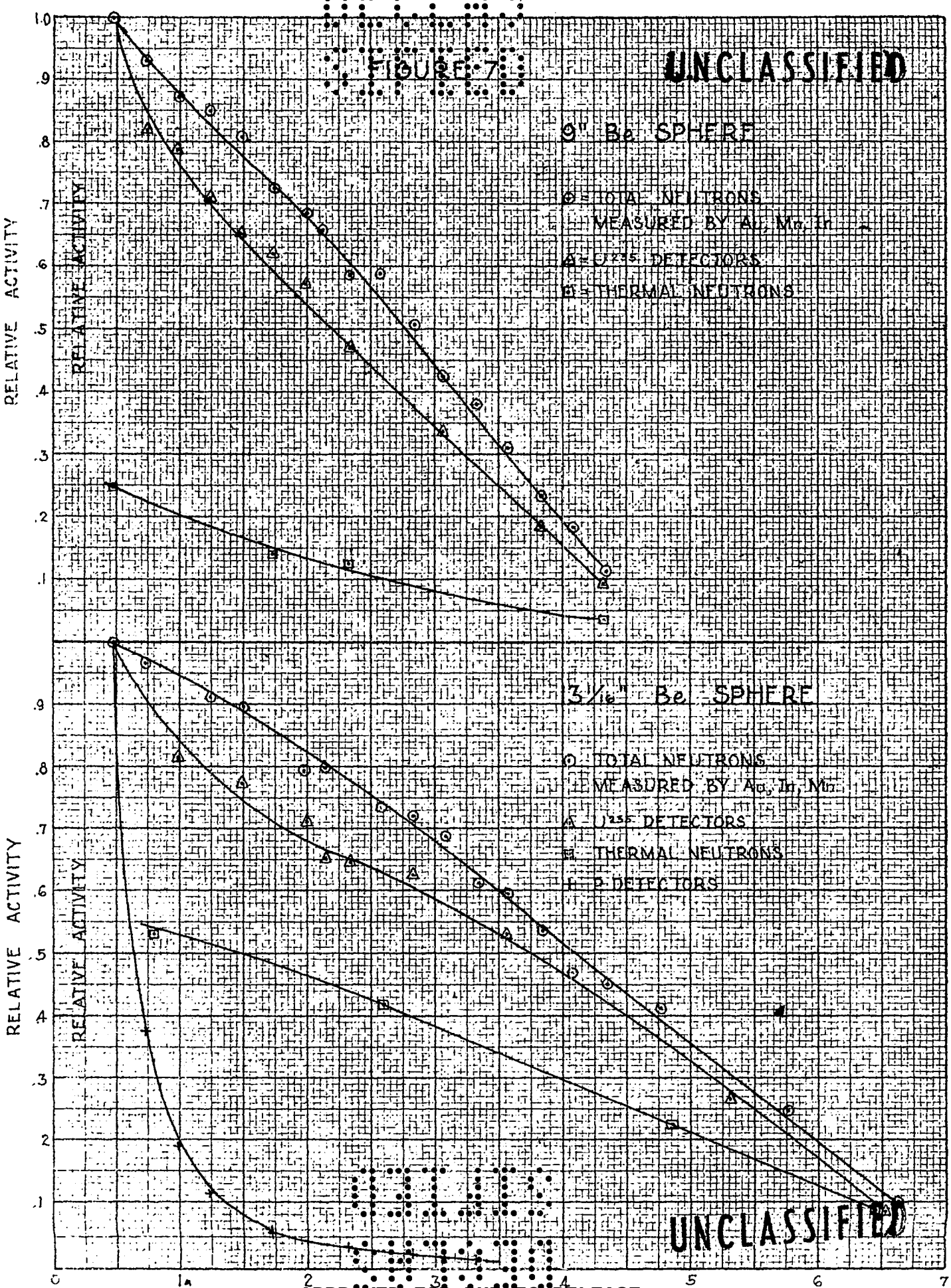

UNCLASSIFIED

APPROVED FOR PUBLIC RELEASE

APPROVED FOR PUBLIC RELEASE

UNCLASSIFIED

FIGURE 8

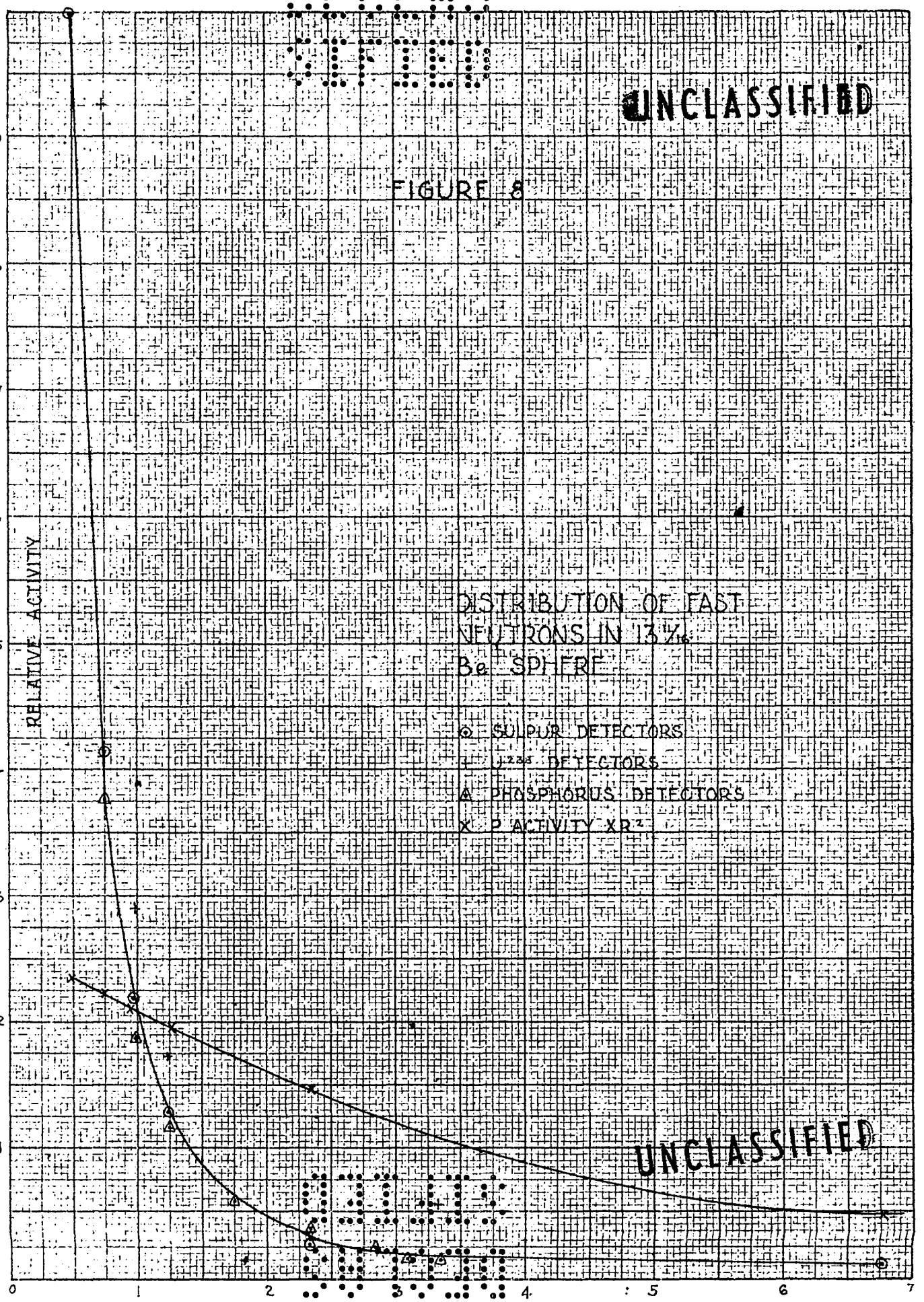

UNCLASSIFIED

APPROVED FOR PUBLIC RELEASE

APPROVED FOR PUBLIC RELEASE

$Po-\alpha-Be$ SOURCE STRENGTH

UNCLASSIFIED

FIGURE 9

SOURCE STRENGTH

$S = 20 \times 10^{7}$ n/sec

$S = 702 \times 10^{6}$ n/sec

SOURCE STRENGTH

10
9
8
7
6
5
4.0
3.0
2.0
1.0
9
8
7
6
5
4
3
2
1

10/19 10/29 11/8 11/18 11/28 12/8 12/18 12/28 1/7 1/17 1/27 2/6 2/16 2/26 3/8

KEUFFEL & ESSER CO., N. Y. NO. 3
MADE IN U.S.A.

UNCLASSIFIED

APPROVED FOR PUBLIC RELEASE

APPROVED FOR PUBLIC RELEASE

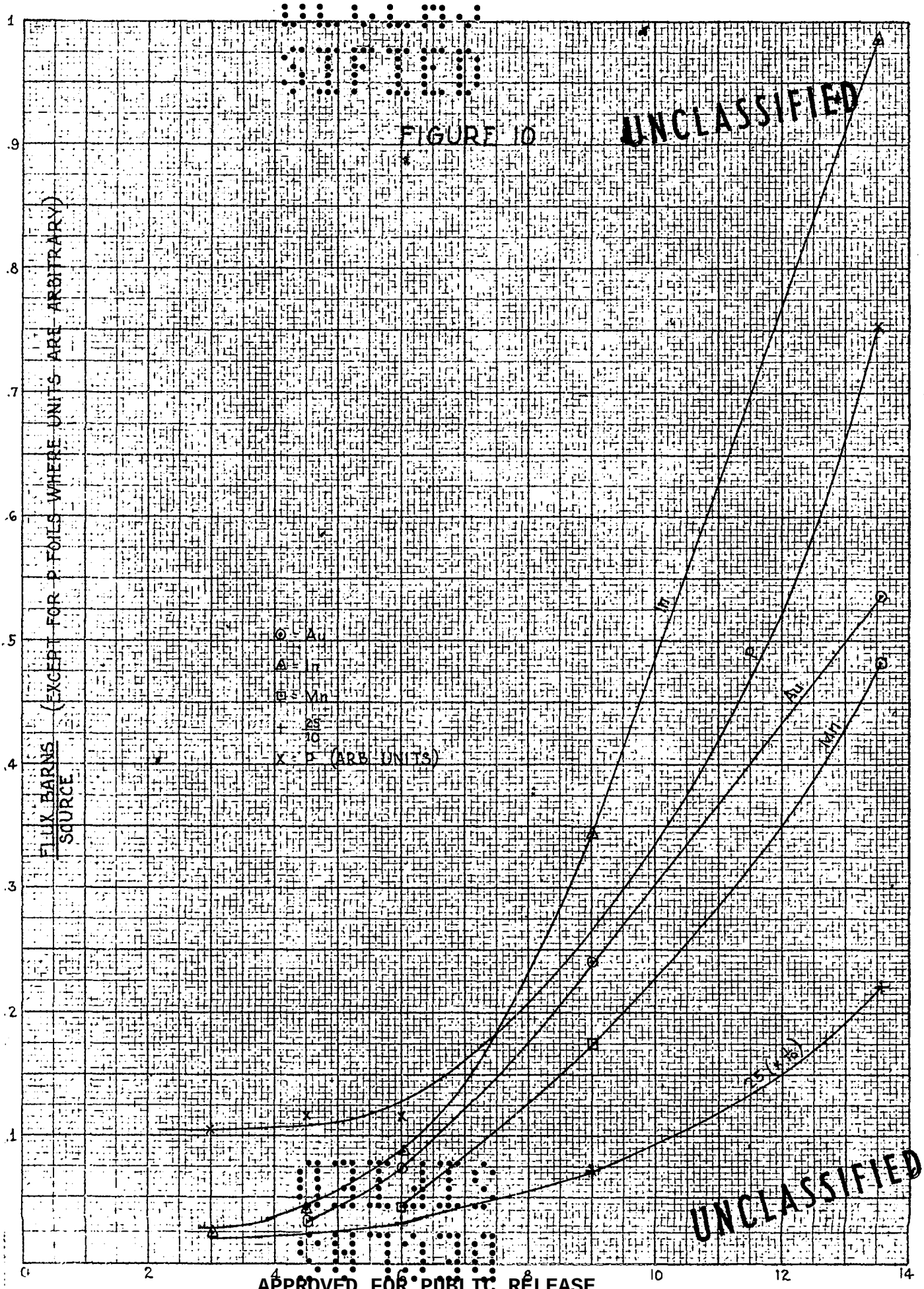

APPROVED FOR PUBLIC RELEASE

APPROVED FOR PUBLIC RELEASE

UNCLASSIFIED

FIGURE 11

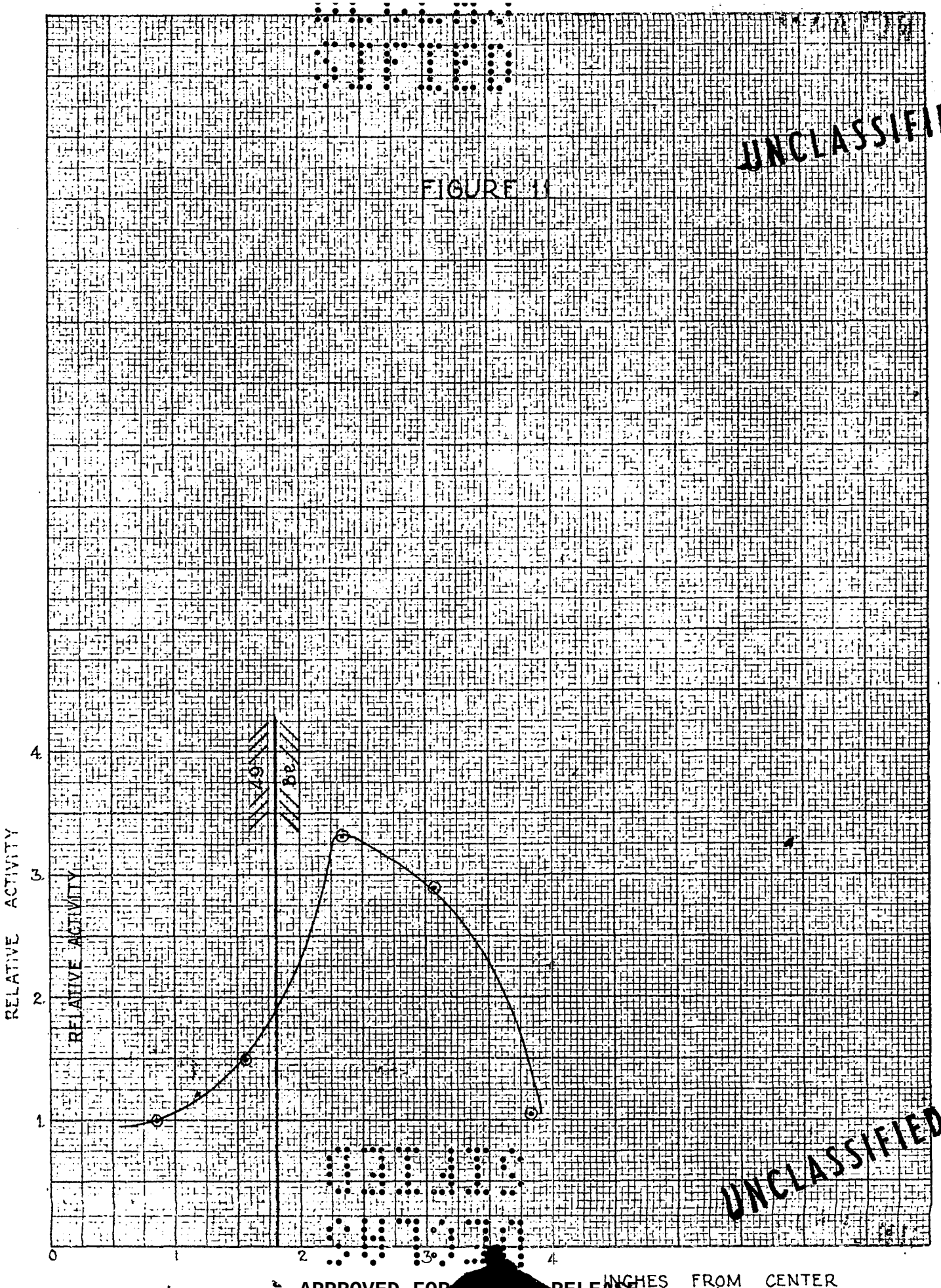

UNCLASSIFIED

APPROVED FOR RELEASE

APPROVED FOR PUBLIC RELEASE

UNCLASSIFIED

DOCUMENT ROOM

REC. FROM GC

DATE 5/31/46

REC. NO. REC. 1

[redacted]

UNCLASSIFIED

APPROVED FOR PUBLIC RELEASE